Trapping and Acceleration in Self-Modulated Laser Wakefields

E. Esarey,[1] B. Hafizi,[2] R. Hubbard,[1] and A. Ting[1]
[1]*Plasma Physics Division, Naval Research Laboratory, Washington, D.C. 20375*
[2]*Icarus Research, Inc., P.O. Box 30780, Bethesda, Maryland 20824-0780*
(Received 10 March 1998)

Trapping of plasma electrons in the self-modulated laser wakefield accelerator via the coupling of Raman backscatter to the wake is examined analytically and with 3D test particle simulations. The trapping threshold for linear polarization is much less than for circular polarization and occurs for wake amplitudes of 25%, which is well below wave breaking. Self-channeling provides continuous focusing of the accelerated electrons, which, along with relativistic pump laser effects, can enhance the energy gain by a factor of ≥ 2. [S0031-9007(98)06509-0]

PACS numbers: 52.75.Di, 41.75.Lx, 41.85.Ar, 52.40.Nk

Plasma-based accelerators [1] are capable of sustaining ultrahigh electric fields E_z in excess of $E_0 = cm\omega_p/e \simeq 97 n_0^{1/2}[\mathrm{cm}^{-3}]$ V/m, where $\omega_p = (4\pi n_0 e^2/m)^{1/2}$ is the plasma frequency and n_0 is the ambient plasma density. Several recent experiments [2–6] have demonstrated the self-trapping and acceleration of plasma electrons in the self-modulated laser wakefield accelerator (SMLWFA) [1,7,8], with electron energies as high as 100 MeV [5,6] over a distance $\sim$2 mm. In the SMLWFA, n_0 is sufficiently high ($n_0 \sim 10^{19}$ cm^{-3}, $E_0 \sim 300$ GV/m) that the laser pulse extends over many plasma wavelengths $\lambda_p = 2\pi c/\omega_p$ ($\lambda_p/\lambda \sim 8$, where $\lambda = 2\pi c/\omega$ is the laser wavelength). A large amplitude plasma wave (wakefield) is generated via a self-modulation or Raman forward scattered (RFS) instability [9] with a phase velocity v_p near the group velocity v_g of the laser pulse, $v_p \simeq v_g$, and $\gamma_p \simeq \gamma_g = (1 - v_g^2/c^2)^{-1/2} \simeq \lambda_p/\lambda$. The wakefield rapidly grows to extreme values such that electrons are self-trapped from the background plasma. Furthermore, the maximum electron energies observed in experiments [5,6] and simulations [6,10] are in excess of the standard dephasing limit [10,11], $W_d \simeq 2\gamma_p^2 mc^2$ ($W_d \sim 65$ MeV).

It has been suggested that wave breaking is the mechanism for self-trapping [2,6,10]. Wave breaking of a cold plasma wave in 1D occurs at [12] $E_{\mathrm{WB}} = [2(\gamma_p - 1)]^{1/2} E_0 \gg E_0$. Thermal and 3D effects can lower this value, but typically wave breaking requires nonlinear plasma waves with $E_z > E_0$ [13]. The observed wakefield amplitude [14], however, is in the range $E_z/E_0 \sim 10\%$–30%, well below the wave breaking limit. Accelerated electrons have also been observed with no evidence of wave breaking, i.e., no broadening of the anti-Stokes peaks [5]. Wave breaking has been suggested as the mechanism by which the electron energies exceed the dephasing limit [6,10].

In this Letter, it is shown that self-trapping and acceleration can result from the coupling of Raman backscattering (RBS) to the wakefield. Self-trapping is found to occur at modest wakefield amplitudes, $E_z/E_0 \simeq 25\%$, on the order of those observed experimentally, and much lower than the cold 1D wave breaking limit, which is shown to be $E_{\mathrm{WB}} = [2\gamma_{\perp 0}(\gamma_p - 1)]^{1/2} E_0$, where $\gamma_{\perp 0} = (1 + a_0^2)^{1/2}$, $a_0^2 \simeq 3.6 \times 10^{-19}\lambda^2[\mu\mathrm{m}] I[W/\mathrm{cm}^2]$ (circular polarization), and I is the laser intensity. It is also shown that the self-trapping threshold is considerably lower for a linearly polarized laser pulse as compared with circular polarization. By including the space-charge field due to self-channeling, it is shown that the maximum energy gain is $W_{\max} = 4\gamma_p^2 mc^2$. Nonlinear effects can further increase $W_{\max}$ by a factor of $F_{NL} \simeq (\gamma_{\perp 0} n_0/n)^{2/3} \sim 3$, where n is the self-channeled density. This can account for the final energies observed in experiments and simulations. Test particle simulations of self-trapping in 3D indicate a large number (10^9) of relativistic electrons with a 100% energy spread and a low normalized emittance, $\epsilon_n \sim 1$ mm mrad.

As the pump laser self-modulates, it also undergoes RBS, which is the fastest growing laser-plasma instability [1,15–18]. RBS is observed in intense short pulse experiments, with reflectivities as high as 10%–30% [15]. RBS generates redshifted backward light of frequency $\omega_0 - \omega_p$ and wave number $-k_0$, which beats with the pump laser (ω_0, k_0) to drive a ponderomotive wave $(\omega_p, 2k_0)$. As the instability grows, the RBS beat wave, which has a slow phase velocity $v_p \simeq \omega_p/2k_0 \ll c$, can trap and heat background plasma electrons [16]. These electrons can gain sufficient energy and/or be displaced in phase by the RBS beat wave such that they are trapped and accelerated to high energies in the wakefield [1,5]. A similar two-stage acceleration process involving the coupling of RFS and RBS has been simulated in 1D by Bertrand *et al.* [17], however, in a much different regime with high density (2×10^{20} cm^{-3}, $\omega_0/\omega_p = 2.36$), low intensity (10^{16} W/cm^2), and high temperature (10 keV) at which the effects of strong Landau damping are important.

To analyze self-trapping, the motion of test particles in analytically specified fields is studied. The effects of four fields will be considered: (1) the intense pump laser field $\mathbf{a}_0$, (2) the RBS radiation field $\mathbf{a}_1$, (3) the plasma wakefield ϕ_p, and (4) the self-channeling space-charge field ϕ_s, where $\phi = e\Phi/mc^2$ and $\mathbf{a} = e\mathbf{A}_\perp/mc^2$ are the

 0031-9007/98/80(25)/5552(4)$15.00

normalized scalar and vector potentials, respectively. Once the fields are specified, the electron motion is evolved via the relativistic Lorentz equation $d\mathbf{u}/dct = \nabla\phi + \partial\mathbf{a}/\partial ct - \beta \times (\nabla \times \mathbf{a})$, where $\mathbf{u} = \mathbf{p}/mc$ is the normalized electron momentum, $\beta = \mathbf{u}/\gamma$, and $\gamma = (1 + u^2)^{1/2}$.

The pump laser ($i = 0$) and RBS radiation ($i = 1$) fields are assumed to be of the form $\mathbf{a}_i = \hat{a}_i(\zeta_i, r)\,(\sin\psi_i \mathbf{e}_x + \sigma\cos\psi_i \mathbf{e}_y) + a_{zi}\mathbf{e}_z$, where $\zeta_i = z - v_{gi}t, \psi_i = k_i z - \omega_i t, v_{g0} = c\beta_{g0} = c^2 k_0/\omega_0$ is the group velocity, $\sigma = 0\,(\sigma = 1)$ for linear (circular) polarization, and $\nabla \cdot \mathbf{a}_i = 0$. The wave numbers k_i and frequencies ω_i satisfy $ck_i = \delta_i\omega_i(1 - \omega_p^2/\omega_i^2 - 4c^2/r_i^2\omega_i^2)^{1/2}$ with $\delta_0 = 1$ (pump) and $\delta_1 = -1$ (RBS). The wakefield is $\phi_p = \hat{\phi}_p(\zeta_p, r)\cos\psi$, where $\zeta_p = z - v_p t$ and $\psi = (\omega_p/v_p)\zeta_p$. The field envelopes are

$$(\hat{a}_i, \hat{\phi}_p) = (a_i, \phi_0)\exp(-r^2/r_j^2) \times \{1 - \exp[-(\zeta_j - \zeta_{fj})^2/L_j^2]\}, \quad (1)$$

for $\zeta_j \le \zeta_{fj}(j = 0, 1, p)$, where $(a_i, \phi_0), \zeta_{fj}, L_j$, and r_j are constants that determine the amplitude, position of the leading edge, rise time, and spot size of the field, respectively. The average power is $P_i[\mathrm{GW}] \simeq 21.5(1 + \sigma)\,(a_i r_i/\lambda_i)^2$ and equal power comparisons require $(a_i^2)_{\sigma=1} = (a_i^2/2)_{\sigma=0}$. Furthermore, $\omega_1 = \omega_0 - \omega_p$, $v_p = v_{g0} = v_{g1}$, and $r_p^2 = r_0^2/2$ are assumed.

The RBS instability is considered in the strong-pump limit, which is characterized by a large growth rate $\Gamma_1 \gg \omega_p$ and in which the effects of the RBS space-charge field ϕ_1 can be neglected [15,18]. The saturation amplitude [18] of the strong-pump RBS radiation is $a_1 = (\omega_p/\omega_0)^{4/3}G(a_0)$, where G is a function of a_0, e.g., $a_1 \simeq 0.046$ for linear polarization, $a_0 = 2$, and $\omega_0/\omega_p = 8.5$. In the absence of RBS, trapping could be induced by injecting a backward laser field of sufficient intensity [19].

In the long pulse ($L_0 \gg \lambda_p$) SMLWFA regime, the ponderomotive force of the pump laser pulse expels electrons (self-channeling), thus creating an electron density perturbation $\delta n/n_0 = k_p^{-2}\nabla^2\phi_s$ and a space-charge potential [20] via $\nabla\phi_s = \nabla\gamma_{\perp 0}$, i.e., $\phi_s = \gamma_{\perp 0} - 1$, where $\gamma_{\perp 0}^2 = 1 + (1 + \sigma)\hat{a}_0^2/2$. The radial space-charge force leads to enhanced focusing of the accelerated electrons.

It is insightful to consider the effects of each of the waves (wakefield and beat wave) independently. In the absence of RBS ($a_1 = 0$), electron motion in a 1D wakefield is described by the Hamiltonian $H_w = \gamma - \beta_p(\gamma^2 - \gamma_{\perp 0}^2)^{1/2} - \phi(\psi)$, where $\gamma_{\perp 0} = (1 + a_0^2)^{1/2}$ is constant (circular polarization), $\beta_p = v_p/c, \phi = \phi_s + \phi_p, \phi_s = \gamma_{\perp 0} - 1$, and $\phi_p = \phi_0\cos\psi$. In phase space (u_z, ψ), the boundary between trapped and untrapped electron orbits is given by the separatrix $H_w(\beta_z, \psi) = H(\beta_p, \pi)$. The maximum (+) and minimum (−) axial momenta of an electron on the separatrix are

$$u_{w,m} = \gamma_p\gamma_{\perp 0}\{\beta_p(1 + 2\phi_0\gamma_p/\gamma_{\perp 0}) \pm [(1 + 2\phi_0\gamma_p/\gamma_{\perp 0})^2 - 1]^{1/2}\}. \quad (2)$$

In the limits $2\phi_0\gamma_p/\gamma_{\perp 0} \gg 1$ and $\gamma_p \gg 1$, $u_{w,\max} \simeq 4\gamma_p^2\phi_0$, and $u_{w,\min} \simeq \gamma_{\perp 0}^2/4\phi_0 - \phi_0$. Notice that $u_{w,\min}$ increases with increasing a_0, i.e., the stronger the pump laser field, the more difficult it is to trap. The background plasma electrons lie on an untrapped orbit (below the separatrix) u_{zf} given by $H_w(u_{zf}, \psi) = 1$. At wave breaking, the bottom of the separatrix $u_{w,\min}$ coalesces with the electron fluid orbit, $u_{zf} = u_{w,\min}$. It can be shown that this occurs at a wave breaking field of $E_{\mathrm{WB}}/E_0 = [2\gamma_{\perp 0}(\gamma_p - 1)]^{1/2}$, e.g., $E_{\mathrm{WB}}/E_0 = 5.1$ for $\gamma_{\perp 0} = \sqrt{3}$ and $\gamma_p = 8.5$.

In the absence of the wakefield ($\phi_p = 0$), electron motion in a 1D ponderomotive beat wave is described by the Hamiltonian $H_b = \gamma - \beta_{pb}[\gamma^2 - \gamma_\perp^2(\psi_b)]^{1/2} + \phi_s$. Circular polarization is assumed such that $\gamma_\perp^2 = 1 + a_0^2 + a_1^2 + 2a_0a_1\cos\psi_b$, where $\psi_b = (k_0 - k_1)\,(z - v_{pb}t)$ and $v_{pb} = c\beta_{pb} = \omega_p/(k_0 - k_1) \simeq \omega_p/2k_0$ is the beat phase velocity, assuming $\omega_p^2/\omega_0^2 \ll 1$ and $1/k_0^2 r_i^2 \ll 1$. The beat separatrix is given by $H_b(\beta_z, \psi_b) = H_b(\beta_{pb}, 0)$ with maximum and minimum axial momenta of

$$u_{b,m} = \gamma_{pb}\{\beta_{pb}[1 + (a_0 + a_1)^2]^{1/2} \pm 2(a_0a_1)^{1/2}\}. \quad (3)$$

In the combined slow beat wave and the fast wakefield, self-trapping can occur as follows. Below wave breaking (e.g., $\phi_0 < 1$), plasma electrons are oscillating on an untrapped orbit below the wake separatrix, i.e., with insufficient energy to be trapped in the fast ($v_p \simeq c$) wakefield. They can, however, be trapped in the slow ($v_{pb} \ll c$) beat wave. The effect of the beat wave is to displace the electrons in both momentum and phase such that a fraction of the orbits cross the wake separatrix and become trapped. Although the actual orbits in both the wakefield and beat wave are highly nonlinear, an approximate trapping threshold is given by an island overlap condition: Trapping occurs when beat and wake separatrices overlap, i.e., $u_{b,\max} > u_{w,\min}$. Using Eqs. (2) and (3) gives a trapping threshold of

$$\phi_0 > \frac{\gamma_{\perp 0}}{2}\left[\left(1 + \frac{u_{b,\max}^2}{\gamma_{\perp 0}^2}\right)^{1/2} - \beta_p\,\frac{u_{b,\max}}{\gamma_{\perp 0}} - \frac{1}{\gamma_p}\right]. \quad (4)$$

In the limits $\gamma_p \gg 1, \beta_{pb} \ll 1$, and $a_1 \ll 1$, Eq. (4) becomes $\phi_0 > (1 - \beta_{pb})\gamma_{\perp 0}/2 - (a_0a_1)^{1/2}$. The above assumes that, in the presence of the wake, well defined beat wave separatrices exist, $2k_0a_0a_1/\gamma_{\perp 0} > k_p|\phi_0|$. For linear polarization, $\gamma_\perp^2 = 1 + a_0^2\sin^2\psi_0$ oscillates on a fine scale ($\lambda_0/2$) with a phase velocity near c. This creates a "fuzzy" wake separatrix, the bottom of which is given by Eq. (2) with $\gamma_{\perp 0} \to 1$. Hence, it is easier to trap with linear polarization. For example, $a_0 = 1.4$, $\gamma_p = \omega_0/\omega_p = 8.5$ ($\beta_{pb} = 0.063$), and $a_1 = 0.033$ give $u_{b,\max} = 0.54$ and a threshold of $\phi_0 > 0.54$ ($\phi_0 > 0.24$) for circular (linear) polarization.

The 1D theory neglects the effects of transverse focusing. Associated with a 3D wake ϕ_p is a periodic radial field which is $\pi/2$ out of phase with accelerating field, i.e., there exists a phase region of $\lambda_p/4$ that is both accelerating and focusing. If an electron is to remain in this

phase region, it must lie within the "3D separatrix" defined by $H_w(\beta_z, \psi) = H_w(\beta_p, \pi/2)$ with extremum given by $u_{w,\max} \simeq 2\gamma_p^2\phi_0$ and $u_{w,\min} \simeq \gamma_{\perp 0}^2/2\phi_0 - \phi_0/2$, i.e., given by Eq. (2) with the substitution $(\phi_0)_{1D} \rightarrow (\phi_0/2)_{3D}$. Similarly, the threshold for trapping on the 3D separatrix is given by Eq. (4) with $(\phi_0)_{1D} \rightarrow (\phi_0/2)_{3D}$; i.e., it takes a wake twice as large to trap on the 3D separatrix as compared to the 1D separatrix.

In the SMLWFA, additional transverse forces arise from the self-channeling space charge potential ϕ_s, which is focusing for all phases. Hence if $|\nabla_\perp \phi_s| > |\nabla_\perp \phi_p|$, the radial space-charge force dominates the radial wake and an accelerated electron is focused for all phases. This condition implies $\phi_0 < (1 + \sigma)a_0^2 r_p^2/2\gamma_{\perp 0} r_0^2$, e.g., $\phi_0 < 0.58$ for $\sigma = 0$, $a_0^2 = 4$, and $r_p^2 = r_0^2/2$. When this is satisfied, the "1D separatrix" trapping results apply, i.e., Eqs. (2) and (4). Furthermore, the maximum energy gain is $W_{\max} \simeq 4\gamma_p^2\phi_0 mc^2$ which is twice the conventional result W_d. In addition, relativistic pump intensities imply $\phi_0 = \gamma_{\perp 0}^{1/2} E_z/E_0$ and $\gamma_p = \gamma_{\perp 0}^{1/2}\omega_0/\omega_p$. Self-channeling may increase ϕ_0 and γ_p by a factor of $(n_0/n)^{1/2}$. Hence, nonlinear effects may increase $W_{\max}$ by a factor as high as $F_{NL} \simeq (\gamma_{\perp 0} n_0/n)^{3/2} \simeq 3.5$, assuming $\gamma_{\perp 0} = \sqrt{3}$ and $n/n_0 = 3/4$.

Simulations of trapping were performed by pushing test (noninteracting) electrons in analytically specified 1D and 3D fields ($\mathbf{a}_0, \mathbf{a}_1, \phi_p$, and ϕ_s as described above). A short axial segment (typically 1 μm) of stationary electrons (typically 16 000 particles) is initiated in front of the laser pulse and is evolved in the fields via the relativistic Lorentz equation. The simulation parameters were (unless otherwise specified) flattop field amplitudes of $a_0 = 1.4\,(a_0 = 2)$ and $a_1 = 0.033\,(a_1 = 0.046)$ for circular (linear) polarization (equal power), $\omega_0/\omega_p = 8.5\,(n_0 = 1.5 \times 10^{19}\ \mathrm{cm}^{-3}$ for $\lambda_0 = 1\ \mu\mathrm{m})$, $\omega_1 = \omega_0 - \omega_p\ (\beta_{pb} \simeq 0.063)$, $v_p = v_{g0} = v_{g1}$, rise lengths on the field profiles of $L_0 = L_1 = L_p = 4\lambda_p$, and positions of the field fronts of $\zeta_{f0} = 0$ and $\zeta_{f1} = \zeta_{fp} = -\lambda_p$.

Figure 1 shows simulation results for 1D fields for circular (solid curves) and linear polarization (dashed curves). Plotted versus ϕ_0 are the maximum electron energy $W_{\max}$ (open points) and fraction of the initial electrons that become trapped f_{tr} (solid points) after a distance of 2 mm. When trapping occurs, $W_{\max}$ agrees with the expression from 1D theory, Eq. (2) with $\gamma_p = 8.5$. Note that the simple expression for $\gamma_p\phi_0/\gamma_{\perp 0} \gg 1$ significantly underestimates the energy gain, i.e., $W_{\max} \simeq 4\gamma_p^2\phi_0 \simeq 59$ MeV for $\gamma_p = 8.5$ and $\phi_0 = 0.4$ as compared to 73 MeV from Eq. (2). For circular (linear) polarization, trapping occurs for $\phi_0 \geq 0.55\,(\phi_0 \geq 0.2)$, in approximate agreement with theory. A similar sudden onset in trapping was observed when a_1 was increased for fixed ϕ_0.

Figures 2 and 3 show results for linearly polarized 3D fields with $r_0 = r_1 = \sqrt{2}\,r_p = 4\ \mu\mathrm{m}\,(\gamma_p = \gamma_{g0} \simeq 7)$. The initial electrons are loaded in $r \leq r_b = 2\ \mu$m (simulations show electrons at $r > 2\ \mu$m do not trap).

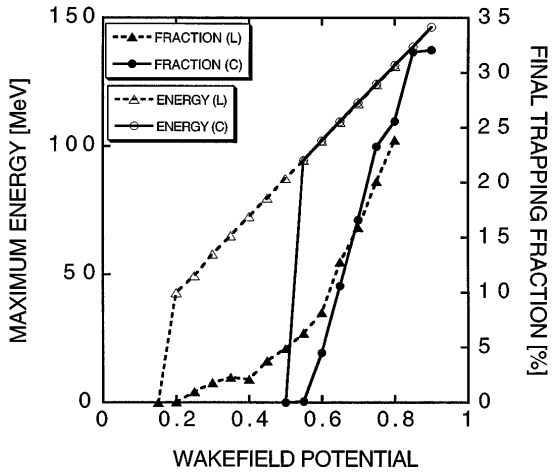

FIG. 1. Maximum electron energy (open points) and trapping fraction (solid points) versus ϕ_0 from 1D simulations with $\omega_0/\omega_p = 8.5$ after 2 mm for circular polarization (solid curves) with $a_0 = 1.4$ and $a_1 = 0.033$ and linear polarization (dashed curves) with $a_0 = 2$ and $a_1 = 0.046$.

Figure 2 shows $W_{\max}$ (solid curve) and f_{tr} (dashed curve) after 1 mm with (a) ϕ_0 varied ($a_1 = 0.046$) and (b) a_1 varied ($\phi_0 = 0.4$). Figure 2(a) shows the onset of trapping at $\phi_0 \simeq 0.2$ (theory gives $\phi_0 \geq 0.23$) and peaks at $\phi_0 \simeq 0.35\,(f_{\mathrm{tr}} \simeq 0.66\%)$. Beyond $\phi_0 \geq 0.6$, trapping is greatly reduced ($f_{\mathrm{tr}} < 0.05\%$), in agreement with theory that predicts radial scattering (defocusing) by the wake when $\phi_0 > 0.58$. A sharp threshold for trapping for sufficiently large a_1 is shown in Fig. 2(b). In the 3D simulations, $W_{\max}$ is slightly higher than the 1D theoretical maximum, e.g., 48 MeV for $\phi_0 = 0.3$ as compared to 41 MeV from theory. For circular polarization, theory predicts trapping when $0.52 < \phi_0 < 0.58$. This behavior is confirmed in 3D simulations which show a narrow band of trapping peaked about $\phi = 0.6$ with $f_{\mathrm{tr}} \simeq 10^{-3}$.

Longitudinal (u_z vs $\zeta = z - ct$) and transverse (β_x vs ζ) electron phase spaces are shown in Figs. 3(a) and 3(b), respectively, for a 3D linearly polarized run with $\phi_0 = 0.3$ after 0.5 mm of propagation. The high energy electrons are confined to $r \leq 1\ \mu$m with a 100% energy spread, $W_{\max} \simeq 47$ MeV, $f_{\mathrm{tr}} \simeq 0.6\%$, and rms normalized emittance $\epsilon_n \simeq (0.5)\pi$ mm mrad.

The test particle simulations neglect several effects such as the self-consistent evolution of the fields, space-charge effects of the accelerated electrons, and beam loading effects. For example, Raman sidescatter will introduce additional waves with $v_p < c$ which will further enhance trapping. Beam loading degrades the wakefield when the total number of trapped electrons N_T approaches the beam loading limit [21] $N_{\max} \simeq n_0(\lambda_p r_0^2/2)E_z/E_0$. In the simulations, $N_T = f_{\mathrm{tr}} n_0 \pi r_b^2 L_p$, where L_p is the propagation length and $r_b = 2\ \mu$m. For the parameters $n_0 = 1.5 \times 10^{19}\ \mathrm{cm}^{-3}$, $\lambda_p = 8.5\ \mu$m, $r_0 = 4\ \mu$m, $f_{\mathrm{tr}} = 0.5\%$, and $E_z/E_0 = 0.5$, the beam loading limit $N_T \simeq N_{\max} \simeq 5 \times 10^8$ is reached after $L_p \simeq 0.5$ mm.

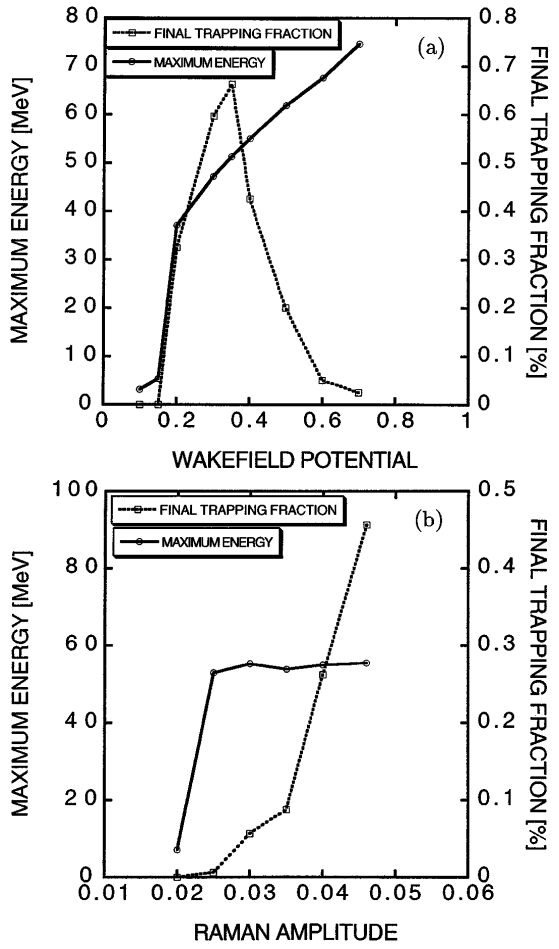

FIG. 2. Maximum energy (solid curve) and trapping fraction (dashed curve) from 3D simulations with linear polarization, $a_0 = 2, \omega_0/\omega_p = 8.5, r_0 = 4\ \mu$m, after 1 mm (a) versus ϕ_0 with $a_1 = 0.046$ and (b) versus a_1 with $\phi_0 = 0.4$.

In summary, trapping and acceleration of plasma electrons in the SMLWFA via the coupling of RBS to the wake has been examined analytically and with 3D test particle simulations. A sudden onset in trapping is observed when either a_1 or ϕ_0 exceeds a threshold. The trapping threshold for linear polarization is much less than that for circular polarization. This threshold occurs well below wave breaking, e.g., $E_z/E_0 \sim 25\%$, consistent with experimental observations. Self-channeling provides continuous focusing of the accelerated electrons which, along with relativistic pump laser effects, can enhance the energy gain by a factor of 2–7. This results in a large number (10^9) of short pulse (<1 ps), relativistic (50 MeV) electrons with 100% energy spread and low emittance ($\epsilon_n < 1$ mm mrad) generated over a short distance (<1 mm).

This work was supported by the Department of Energy and the Office of Naval Research.

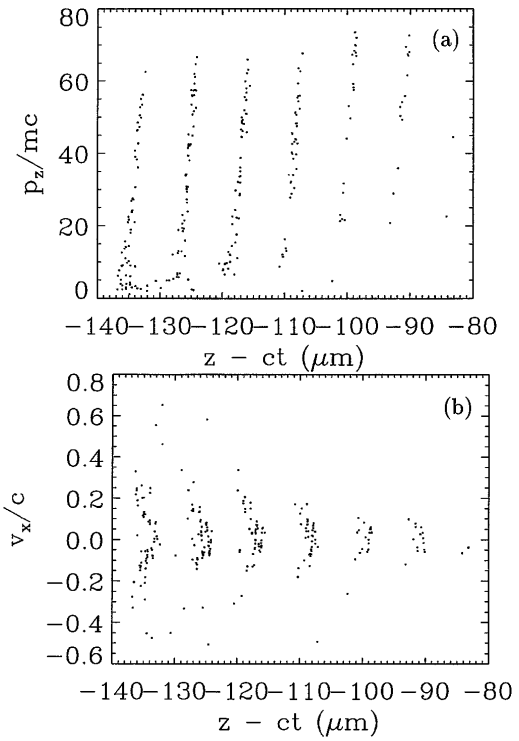

FIG. 3. (a) Longitudinal (u_z vs $z - ct$) and (b) transverse (β_x vs $z - ct$) phase spaces from a 3D simulation with linear polarization, $a_0 = 2$, $\omega_0/\omega_p = 8.5$, $r_0 = 4\ \mu$m, $a_1 = 0.046$, $\phi_0 = 0.3$, after 0.5 mm.

[1] For a review, see E. Esarey *et al.*, IEEE Trans. Plasma Sci. **PS-24**, 252 (1996).
[2] A. Modena *et al.*, Nature (London) **377**, 606 (1995).
[3] K. Nakajima *et al.*, Phys. Rev. Lett. **74**, 4428 (1995); C. Coverdale *et al.*, Phys. Rev. Lett. **74**, 4659 (1995).
[4] D. Umstadter *et al.*, Science **273**, 472 (1996); R. Wagner *et al.*, Phys. Rev. Lett. **78**, 3125 (1997).
[5] A. Ting *et al.*, Phys. Plasmas **4**, 1889 (1997); C. I. Moore *et al.*, Phys. Rev. Lett. **79**, 3909 (1997).
[6] D. Gordon *et al.*, Phys. Rev. Lett. **80**, 2133 (1998).
[7] P. Sprangle *et al.*, Phys. Rev. Lett. **69**, 2200 (1992); E. Esarey *et al.*, Phys. Fluids B **5**, 2690 (1993).
[8] T. M. Antonsen and P. Mora, Phys. Rev. Lett. **69**, 2204 (1992); N. E. Andreev *et al.*, JETP Lett. **55**, 571 (1992).
[9] W. B. Mori *et al.*, Phys. Rev. Lett. **72**, 1482 (1994); E. Esarey *et al.*, Phys. Rev. Lett. **72**, 2887 (1994).
[10] K. C. Tzeng *et al.*, Phys. Rev. Lett. **79**, 5258 (1997).
[11] T. Tajima and J. M. Dawson, Phys. Rev. Lett. **43**, 267 (1979).
[12] A. I. Akhiezer and R. V. Polovin, Sov. Phys. JETP **3**, 696 (1956).
[13] T. Katsouleas and W. B. Mori, Phys. Rev. Lett. **61**, 90 (1988); S. V. Bulanov *et al.*, Phys. Rev. Lett. **78**, 4205 (1997).
[14] A. Ting *et al.*, Phys. Rev. Lett. **77**, 5377 (1996); S. P. LeBlanc *et al.*, Phys. Rev. Lett. **77**, 5381 (1996).
[15] C. Rousseaux *et al.*, Phys. Rev. Lett. **74**, 4655 (1995); A. Ting *et al.*, Opt. Lett. **21**, 1096 (1996).
[16] C. Joshi *et al.*, Phys. Rev. Lett. **47**, 1285 (1981).
[17] P. Bertrand *et al.*, Phys. Plasmas **2**, 3115 (1995).
[18] E. Esarey and P. Sprangle, Phys. Rev. A **45**, 5872 (1992).
[19] E. Esarey *et al.*, Phys. Rev. Lett. **79**, 2682 (1997).
[20] For a review, see E. Esarey *et al.*, IEEE J. Quantum Electron. **33**, 1879 (1997).
[21] T. Katsouleas *et al.*, Part. Accel. **22**, 81 (1987).